Characterisation of Four New Two-Dimensional Lithium Beryllofluoro-Layered Compounds

Lee A. Gerrard* and Mark T. Weller[a]

Abstract: Four new amine-templated materials, containing two-dimensional lithium beryllofluoride sheets of the stoichiometry $[LiBeF_4]^-$, have been synthesised under hydrothermal and ambient pressure conditions. $[LiBeF_4][C_6H_4(CH_3)CH_2NH_3]$ (**1**), $[LiBeF_4][C_6H_4CH_2NH_3Cl]$ (**2**), $[LiBeF_4]_2[NH_3CH_2CH_2CH_2NH_3]$ (**3**), and $[LiBeF_4][C_6H_5CH_2CH_2CH_2NH_3]$ (**4**) all contain well-separated anionic sheets containing two different topologies with the 'inter-layer' regions comprising of organoamine templating species. Use of the different organoamine templating agents results in compounds possessing very different relative arrangements of the lithium beryllofluoride sheets. The materials crystallise in P-centred orthorhombic and monoclinic cells; for **1** (templating agent: 3-methylbenzylamine) P$ca2_1$; for **2** (4-chlorobenzylamine) P*bca*; for **3** (1,3-diamminopropane) P*ccn*, and for **4** (3-phenyl-1-propylamine) P$2_1/c$. Hydrogen bonding exists between ions situated on the protonated amine groups on the templating species and electronegative fluoride ions, on MF_4 tetrahedra (where M = Li and Be).

Keywords: beryllium · hydrothermal synthesis · layered compounds · lithium · template synthesis

Introduction

Materials assembled from tetrahedral units are presently of interest due to the variety of properties the resultant frameworks can exhibit, including porosity, ion-exchange selectivity and electronic/magnetic behaviours. The majority of materials in this class are metal-oxide frameworks, as in zeolites[1, 2] (aluminosilicates), aluminophosphates[3, 4] and some transition-metal phosphates.[5, 6] Formation of these frameworks usually requires the presence of a specific templating species to direct the adoption of a particular structural topology. Materials with varying dimensionality, such as 1D chains,[7] 2D sheets[8] and 3D networks,[9] have been synthesised through variation of the shape and functionality of the templating agent. Many of these oxide-based materials have been synthesised by using a vast array of organoamine templating species.[10–12]

Very few one-, two- and three-dimensional framework compounds constructed from MF_4 tetrahedral building units are known. Formulation of these fluoride-based analogues requires lower charged metallic species, such as M^{2+} and M^+, to counterbalance the decreased negative charge from the fluoride ions, that is -1 compared to -2 from oxide ions. A prerequisite for materials to preserve the tetrahedral topology is to prevent the cation expansion to five or six; therefore, metals with small cations such as lithium, beryllium and boron are ideal candidates for fluoride-based frameworks.

The previously reported 1D[13] and 2D[14] amine-templated materials, formally possessing linked BeF_4 and LiF_4 tetrahedra, have been synthesised by using hydrothermal methods. The use of these conditions is prevalent for the construction of zeotype materials because it not only encourages the synthesis of condensed frameworks but also the formation of good quality single crystals. The 1D material $[LiBe_2F_7][C_4N_2H_{12}][H_2O]_{1.5}$ has a connectivity of two linked strands of BeF_4 and LiF_4 tetrahedra, which produces a corner-sharing 'double' chain with each metal bonded through doubly bridging fluoride ions. The chains run parallel to each other and are encircled by organoamine and solvent water molecules. In addition we have described previously the 2D sheet materials, $[Li_2Be_2F_8][C_2N_2H_{10}]$ and $[Li_2Be_2F_8][CH_3NH_3]_2[H_2O]_2$, that were synthesised by using ethylenediamine[14] and methylamine,[14] respectively. The topology is based on parallel rows of T4 and T3 'ladders', with the T4 rings edge-sharing in a 'double-diamond' motif.[15] The sheets pack parallel to each other and are hydrogen-bonded to templating species that line the inter-layer regions.

Herein we describe four new fluoro-tetrahedral compounds; two that contain a 2D architecture with a layered structure and two that have the same 2D inorganic sheet topology as those in reference [14]. Compounds $[LiBeF_4][C_6H_4(CH_3)CH_2NH_3]$ (**1**), $[LiBeF_4][C_6H_4CH_2NH_3Cl]$

[a] Dr. L. A. Gerrard, Prof. M. T. Weller
Department of Chemistry,
University of Southampton (UK)
Fax: (+44) 23-80-59-6805
E-mail: lag4@soton.ac.uk

Supporting information for this article is available on the WWW under http://www.wiley-vch.de/home/chemeurj.org/ or from the author.

DOI: 10.1002/chem.200304991

(**2**) and $[LiBeF_4][C_6H_5CH_2CH_2CH_2NH_3]$ (**4**) were synthesised by using hydrothermal conditions, whereas compound $[LiBeF_4]_2[NH_3CH_2CH_2CH_2NH_3]$ (**3**) was synthesised by a two-step hydrothermal and slow evaporation process.

Results and Discussion

Single-crystal X-ray analysis (Figure 1a and b) shows that compounds $[LiBeF_4][C_6H_4(CH_3)CH_2NH_3]$ (**1**) and $[LiBeF_4][C_6H_4CH_2NH_3Cl]$ (**2**) both consist of a novel 2D lithium beryllofluoride sheet with bulky amine-templating agents lying in the inter-layer spacing. In the basic unit of **1** and **2**, the Li^{I} and Be^{II} centres occupy distorted tetrahedral geometries, both coordinated to terminal, doubly and triply bridging fluoride ions. Each beryllium atom is bonded to a single terminal fluoride ion F1, two doubly bridged fluoride ions F2 and F3, and a triply bridging fluoride ion F4. The Be–F bond lengths range from 1.533(3) to 1.549(3) Å in **1** and from 1.516(7) to 1.560(8) Å in **2**, and the F-Be-F angles vary from 105.7(2) to 111.1(2)° in **1** and from 104.6(5) to 111.2(5)° in **2**. Each lithium atom is bonded to two doubly (F2 and F3) and two triply bridging fluoride ions (both F4). The Li–F bond lengths range from 1.863(4) to 1.947(4) Å for **1** and from 1.876(10) to 1.945(10) Å for **2;** the F-Li-F angles are slightly distorted from the ideal values expected for tetrahedra (97.4(2)–123.3(2)° for **1**; 96.2(4) and 127.0(5)° for **2**). These are again in good agreement with geometries for this type of species described previously,[17] (Tables 1 and 2). The triply bridging fluoride has two ′longer′ bonds, both to lithium atoms. These can be seen to connect a ′pseudo′ chain of lithium atoms together, running parallel to the *c* (*b*) axis (value in parentheses is for compound **2**). The triply bridging mode of the fluoride ligand has longer bonds than the terminal and doubly bridged species to the metal ions.

Every BeF_4 tetrahedra is bridged to four LiF_4 units through two doubly bridging and one triply bridging fluoride ion, leaving a terminal fluoride ion which is directed, perpendicular to the sheet, into the inter-layer region. The LiF_4, on the other hand, is connected to two identical LiF_4 units and two BeF_4 moieties through the triply bridging, F4, and also to two

Table 1. Important bond lengths [Å] for **1**–**4** (esds are given in parentheses).[a]

1		**2**		**3**		**4**	
Li–F2^{i}	1.863(4)	Li–F2^{3}	1.876(10)	Li–F1	1.866(4)	Li–F1^{1}	1.877(7)
Li–F3^{ii}	1.881(4)	Li–F3	1.880(11)	Li–F1^{c}	1.873(4)	Li–F1	1.854(7)
Li–F4	1.893(4)	Li–F4^{4}	1.885(9)	Li–F2^{a}	1.828(4)	Li–F2	1.831(7)
Li–F4^{iii}	1.947(4)	Li–F4^{5}	1.945(10)	Li–F4^{b}	1.829(4)	Li–F4	1.877(7)
Be–F1	1.533(3)	Be–F1	1.516(7)	Be–F1	1.571(3)	Be–F1	1.586(6)
Be–F2	1.547(3)	Be–F2	1.559(9)	Be–F2	1.521(3)	Be–F2^{5}	1.536(6)
Be–F3	1.538(3)	Be–F3	1.537(9)	Be–F3	1.550(3)	Be–F3	1.546(6)
Be–F4	1.549(3)	Be–F4	1.560(8)	Be–F4	1.553(3)	Be–F4^{2}	1.545(6)

[a] Symmetry transformations used to generate equivalent atoms: For **1**: i: $2-x, 1-y, 1/2+z$; ii: $x-1/2, 1-y, z$; iii: $3/2-x, y, 1/2+z$. For **2**: 3: $-x-1/2, y+1/2, z$; 4: $x-1/2, y, -z+1/2$; 5: $-x, y+1/2, -z+1/2$. For **3**: a: $-x+1, -y, -z$; b: $x, y-1, z$; c: $-x+1, y-1/2, -z+1/2$. For **4**:**1**: $-x, y-1/2, -z+3/2$; **2**: $-x, -y+1, -z+2$; **5**: $x, y+1, z$.

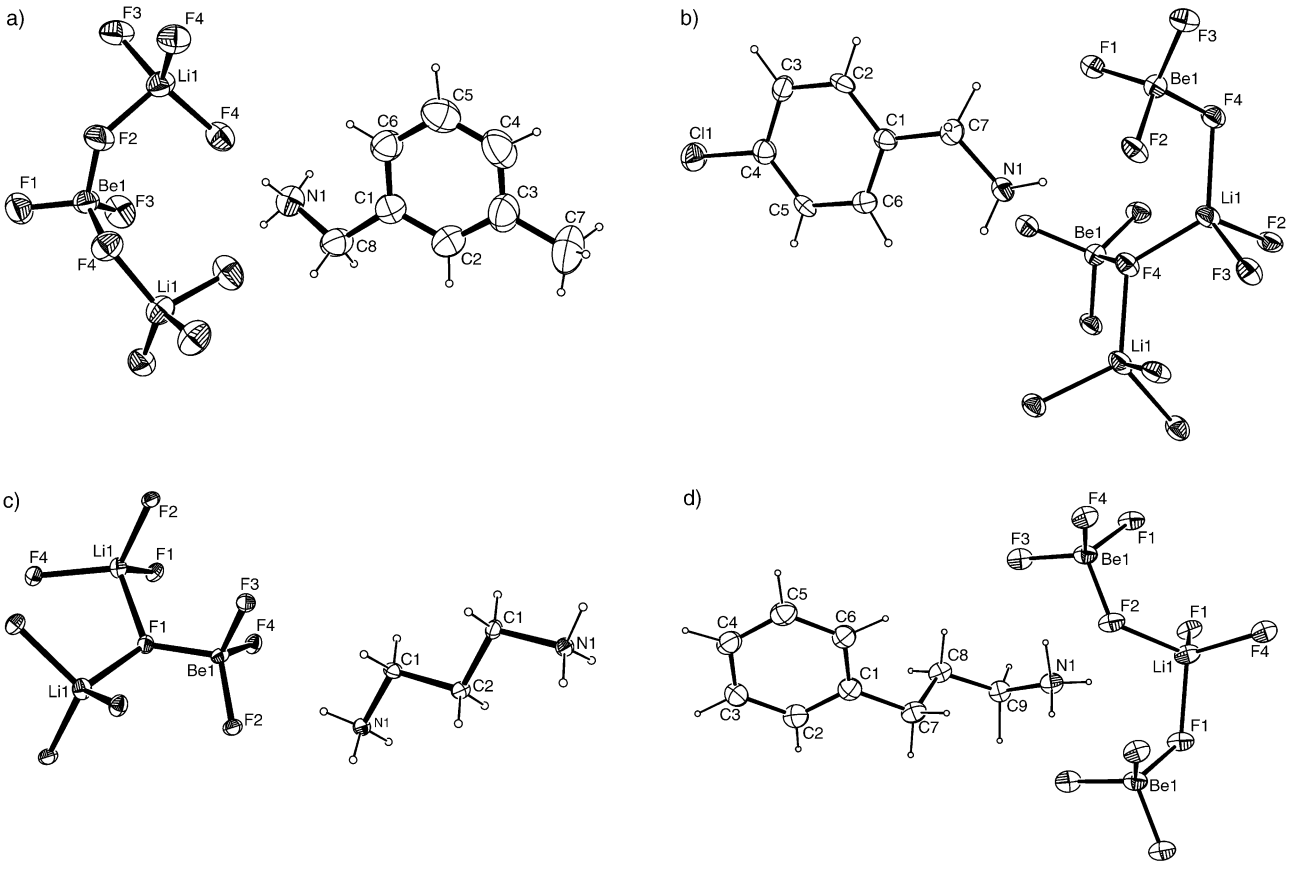

Figure 1. Small segment of the 2D sheet and organoamine templating moiety of compounds **1**–**4** (thermal ellipsoid plot, 50% probability). Templating moiety: a) 3-methylbenzylamine, b) 4-chlorobenzylamine, c) 1,3-diaminopropane, and d) 3-phenyl-1-propylamine.

Table 2. Important bond angles [°] for **1**–**4** (esds are given in parentheses).[a]

1		**2**		**3**		**4**	
F2^{i}-Li-F3^{ii}	97.38(16)	F2^{3}-Li-F3	96.2(4)	F1-Li-F1^{c}	103.2(2)	F1-Li-F1^{1}	104.1(3)
F2^{i}-Li-F4	105.10(20)	F2^{3}-Li-F4^{4}	103.3(5)	F2^{a}-Li-F1	110.3(2)	F2-Li-F1	108.3(3)
F2^{i}-Li-F4^{iii}	101.10(19)	F2^{3}-Li-F4^{5}	99.1(5)	F2^{a}-Li-F4^{b}	120.5(2)	F2-Li-F4	118.6(4)
F3^{ii}-Li-F4	104.30(20)	F3-Li-F4^{4}	104.5(5)	F2^{a}-Li-F1^{c}	108.0(2)	F2-Li-F1^{1}	105.3(3)
F3^{ii}-Li-F4^{iii}	123.30(20)	F3-Li-F4^{5}	127.0(5)	F4^{b}-Li-F1	106.6(2)	F4-Li-F1	109.8(3)
F4-Li-F4^{iii}	121.19(17)	F4^{4}-Li-F4^{5}	120.5(5)	F4^{b}-Li-F1^{c}	106.8(2)	F4-Li-F1^{1}	109.6(3)
F1-Be-F2	109.40(20)	F1-Be-F2	109.8(5)	F1-Be-F2	110.0(2)	F1-Be-F2^{5}	107.3(3)
F1-Be-F3	110.23(18)	F1-Be-F3	110.9(5)	F1-Be-F3	108.6(2)	F1-Be-F3	108.4(4)
F1-Be-F4	110.15(15)	F1-Be-F4	110.1(5)	F1-Be-F4	107.5(2)	F1-Be-F4^{2}	109.7(3)
F2-Be-F4	105.68(18)	F2-Be-F4	104.6(5)	F2-Be-F4	108.6(2)	F2^{5}-Be-F4^{2}	108.4(4)
F3-Be-F2	110.15(15)	F3-Be-F2	110.1(5)	F3-Be-F2	113.9(2)	F3-Be-F2^{5}	109.5(3)
F3-Be-F4	111.10(20)	F3-Be-F4	111.2(5)	F3-Be-F4	108.0(2)	F3-Be-F4^{2}	113.3(3)

[a] Symmetry transformations used to generate equivalent atoms: For **1**: i: $2-x$, $1-y$, $1/2+z$; ii: $x-1/2$, $1-y$, z; iii: $3/2-x$, y, $1/2+z$. For **2**: 3: $-x-1/2$, $y+1/2$, z; 4: $x-1/2$, y, $-z+1/2$; 5: $-x$, $y+1/2$, $-z+1/2$. For **3**: a: $-x+1$, $-y$, $-z$; b: x, $y-1$, z; c: $-x+1$, $y-1/2$, $-z+1/2$. For **4**: **1**: $-x$, $y-1/2$, $-z+3/2$; **2**: $-x$, $-y+1$, $-z+2$; **5**: x, $y+1$, z.

more BeF_4 tetrahedra through the doubly bridging fluoride ions. This connectivity forms a 2D sheet topology with chains of corner-sharing LiF_4 tetrahedra, running perpendicular to the *b* (*c*) axis.

The 1D chains are interlaced above and below with BeF_4 ′bridging′ blocks, which alternate by pointing above and below the plane of the sheet, to form a layer composed of both T3 and T4 rings (Figure 2a and c). This layer undulates with solely BeF_4 moieties positioned at the peaks and troughs, and LiF_4 units lying, between the peaks and troughs, on the same plane running perpendicular to the *b* (*c*) axis. The sheet can be viewed in two ways; firstly as parallel edge-sharing ′ladders′ of T4 and T3 nets running diagonally across the layer or secondly as a chain of ′diamond′ corner-sharing 4-nets, running parallel to the *c* (*b*) axis, linked to adjacent chains by a -F-Li-F-Li-F- connected sequence.

The topology adopted by the anionic sheet is presumably a response to the structure-directing effect of the position of the terminal -NH_3 group on the templating agents. In compounds **1** and **2** the protonated amine group, which lies perpendicular to the layer, is positioned at the centre of four adjacent BeF_4 ′peaks′ on the sheet, and therefore lies almost directly above a ′trough′ (see schematic representation in Figure 3 a and b). All the hydrogen atoms on the -NH_3 unit are involved in

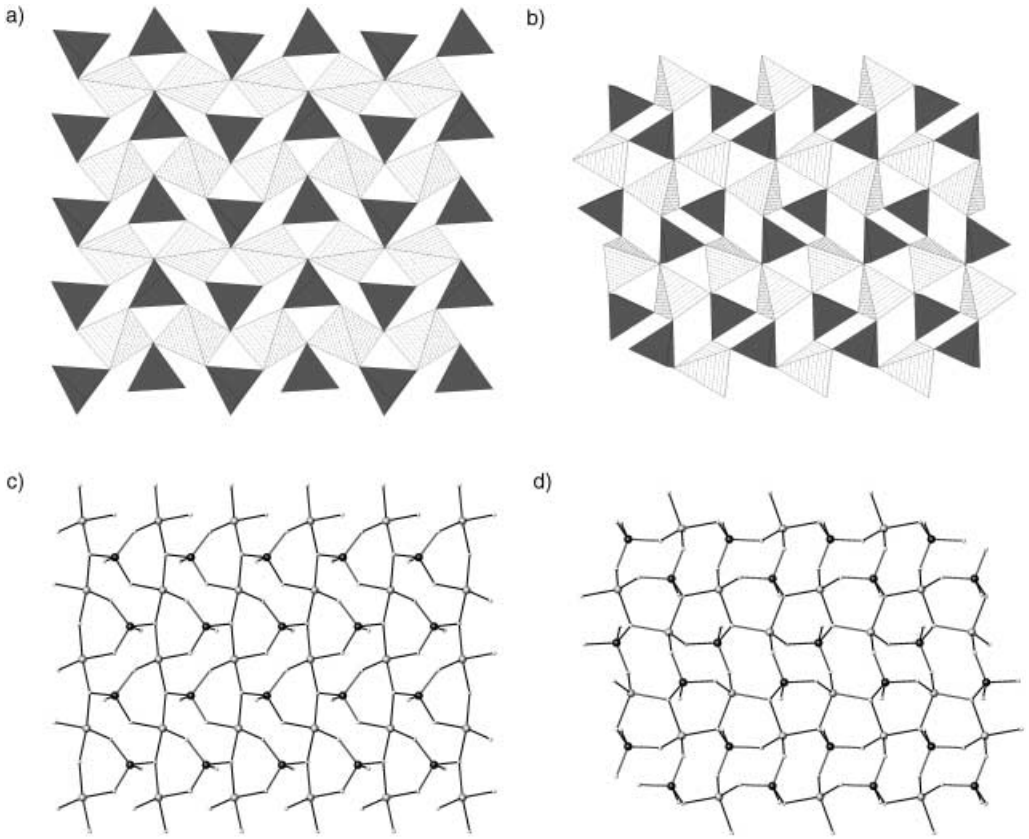

Figure 2. Schematic representations of the two anionic 2D layers; a) Polyhedral representation of **1** and **2**. b) Polyhedral representation of **3** and **4**. Code: light hatched tetrahedra: LiF_4; dark tetrahedra: BeF_4. c) T-F-T connectivity representation of **1** and **2**. d) T-F-T connectivity representation of **3** and **4**. Code: large light spheres: lithium atoms; large dark spheres: beryllium atoms; small light grey spheres: fluorine atoms.

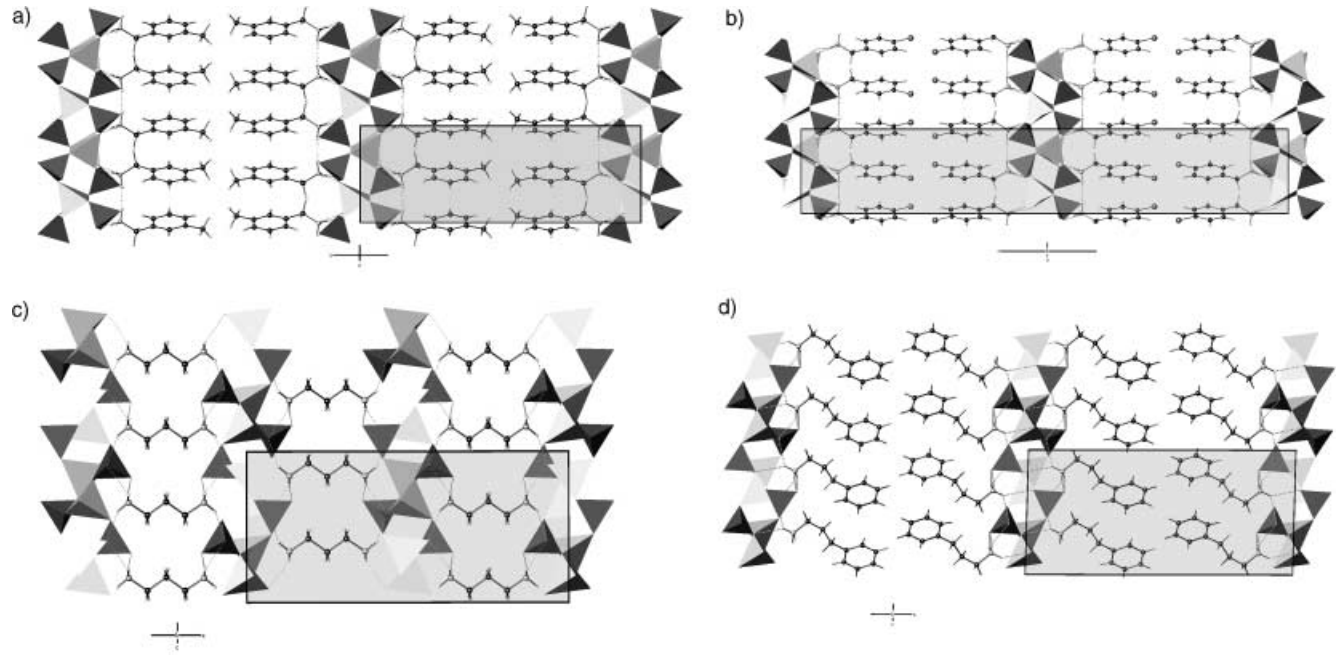

Figure 3. Packing diagram showing the 2D anionic layers interspersed with the columns of the organoamine templates. Both the non-polar and the hydrogen bonding is clearly shown. a) **1**; b) **2**; c) **3**; d) **4**. Code: light polyhedra: LiF_4; dark polyhedra: BeF_4; dark spheres: carbon; light spheres: nitrogen; small hollow spheres: hydrogen. Hydrogen bonding is shown as dashed lines.

hydrogen bonding, one to a terminal and two to doubly bridged fluoride ions. These hydrogen bonds are relatively short (2.711(2), 2.713(3) and 2.722(3) Å for **1;** 2.715(5), 2.722(5) and 2.722(5) Å for **2**, for N–H···F, Table 3). Each 'face' of the tetrahedral sheet, parallel to the *bc* plane, is hydrogen bonded.

Table 3. Hydrogen bonds for compounds **1** and **2** [Å and °].[a]

D–H···A	*d*(D–H)	*d*(H···A)	*d*(D···A)	∢DHA
		1		
N1–H9···F3	0.84(3)	1.90(3)	2.722(3)	164(3)
N1–H10···F2[a]	0.92(3)	1.81(3)	2.713(3)	168(3)
N1–H11···F1[b]	0.94(3)	1.81(3)	2.711(2)	161(3)
		2		
N1–H1A···F3[7]	0.89(5)	1.92(7)	2.722(5)	148.7(5)
N1–H1B···F2	0.89(5)	1.86(7)	2.722(5)	162.9(6)
N1–H1C···F1[8]	0.89(5)	1.87(7)	2.715(5)	158.0(5)

[a] Symmetry transformations used to generate equivalent atoms: a: x, y, $z+1$; b: $-x+3/2$, y, $z+1/2$; 7: x, $y-1$, z; 8: $-x+1/2$, $y-1/2$, z.

In the two compounds the templating agents lie in the 'corrugated' interlayer spacing, which has an average separation of about 21 Å for **1** and about 20 Å for **2**. In both **1** and **2** adjacent inorganic layers, along the *b* and *c* axis, respectively, line up with 'peaks' on one sheet lying opposite troughs on the next layer, producing an AAAAA-type stacking sequence. If viewed down the *a* axis (in both) compound **1** displays an AAAAA packing sequence with all the layers lining up, whereas in **2** alternate layers shift slightly, along the *b* axis, resulting in an ABABA sequence.

In both compounds the interlayer region consists of two columns of the organic moieties, running parallel to the anionic layers. In **1** these two columns are separated by about 2.8 Å, due to the inherent non-polar interactions of the terminal methyl groups in the 3-position on the benzyl ring (Figure 3a). Figure 3a also shows the full hydrogen bonding schematic through the terminal NH_3 groups to the anionic layers. In **2** these two columns are again separated by roughly 3.0 Å, due to the repulsive interactions of adjacent chloride ions in the 4-position. The change in both the position, from the 3- to the 4-position on the benzyl ring, and in the functional group forces adjacent layers, in **2**, to stack in a slightly different topology (Figure 3b).

The structure of compounds **3** and **4** (Figure 1c, d) although having the same $LiBeF_4$ sheet as compounds **1** and **2**, displays a slightly different layer topology. Again, as in **1** and **2**, the sheet is composed of vertex-sharing BeF_4 and LiF_4 tetrahedra with both triply, doubly and terminal fluoride bridging ions. The connectivity of both beryllium and lithium tetrahedra is exactly the same; each BeF_4 unit shares vertices with four LiF_4 moieties through two doubly bridged and one triply bridged fluoride ion, and each LiF_4 tetrahedra bonds to two BeF_4 units through doubly bridged fluoride ions and links to two BeF_4 and two other LiF_4 units each through a triply shared vertex.

The Be–F bond lengths range from 1.521(3) to 1.571(3) Å for **3** and from 1.536(6) to 1.586(6) Å for **4**, and the F-Be-F angles vary from 108.0(2) to 113.9(2)° for **3** and from 107.3(3) to 113.3(3)° for **4**. The Li–F bond lengths range from 1.828(4) to 1.873(4) Å for **3** and from 1.831(7) to 1.877(7) Å for **4**, and the F-Li-F angles are slightly distorted from the ideal values expected for tetrahedra, with values between 103.2(2) and 120.5(2)° for **3** and between 104.1(3) and 118.6(4) for **4**. These are in good agreement with other distances and angles described in the literature[17] (Table 1 and Table 2, and Figure 1 c) and d).

The connectivity of the tetrahedral units in **3** and **4** produce a 2D array that can be illustrated as an infinite sheet of chains

forming parallel ladders of T4 and T3 rings, respectively. The T4 rings edge-share and alternate in a 'double-diamond' motif,[18] and are interspersed, above and below, with rows of triangular cavities, 3-nets, which point in opposing directions (Figure 2 b and d). The 2D sheet again has a corrugated effect with the BeF_4 units at the peaks and troughs and the LiF_4 tetrahedra lying on the same plane bisecting the *a* axis.

The templating agents, 1,3-diaminopropane in **3** and 3-phenyl-1-propylamine in **4**, again influence the structural relationship between the corrugated sheets (Figure 3 c). As before the functional groups on the template nestle in the troughs but in **3** the doubly protonated amine requires two $LiBeF_4$ units, each -1, to balance the overall charge. This smaller diamine with two terminal -NH_3 functional groups produces a contraction of the interlayer spacing (average separation of $a/2 = 10.528$ Å; almost half that observed for **1** and **2**), whereas the inter-layer spacing in **4** is about 21 Å which is again on a par with that of **1** and **2**.

Compound **4** has two columns of organoamine templates in between the anionic sheets, just as **1** and **2**, whereas **3** has just a single row. This is due to the number of NH_3 groups present on the amine. The amine functional groups form hydrogen bonds to the sheets, and therefore the diamine has two separate layers hydrogen-bonded to each (Figure 3 d).

Even though the hydrogen bonding is again through NH_3 groups, as in **1** and **2**, the number of hydrogen bonds is increased by one for **3** and by two for **4**. In compound **3** the two normal hydrogen bonds are 2.799(3) and 2.913(2) Å in length, whereas the bifurcated hydrogen bond (2.880(3) and 3.014(3) Å) is slightly longer, and therefore weaker. Compound **4** has five unique hydrogen bonds for N–H···F distances, two bifurcated to F3 (2.806(5) and 3.097(4) Å) and to F2 (2.906(4) and 2.972(5) Å) and a single very weak normal hydrogen bond to F1 (3.263(5) Å). In compound **3** only two of the four fluoride ions are involved with the hydrogen-bonding interactions, namely the terminal F3 and one of the doubly bridged fluoride ions F4. In contrast, in compound **4**, three fluorides are involved, namely, the terminal F3, the doubly bridged F2 and in addition the very weak hydrogen bonding interaction to the triply bridged fluoride ion F1. All the hydrogen bonding distances for **3** and **4** are given in Table 4.

Table 4. Hydrogen bonds for compounds **3** and **4** [Å and °].[a]

D–H···A	*d*(D–H)	*d*(H···A)	*d*(D···A)	∢DHA
		3		
N1-H1···F3[a]	0.91(3)	1.90(3)	2.799(3)	173(3)
N1–H2···F4[b]	0.93(3)	2.05(3)	2.880(3)	147(2)
N1–H3···F3[c]	0.95(3)	2.08(3)	3.014(3)	169(2)
N1–H3···F4[c]	0.95(3)	2.31(3)	2.913(2)	120(2)
		4		
N1–H1A···F3[3]	1.14(8)	1.99(8)	3.097(4)	162(6)
N1–H1A···F2	1.14(8)	2.14(7)	2.906(4)	121(5)
N1–H1B···F3	0.86(5)	1.95(6)	2.806(5)	169(4)
N1–H1C···F2[6]	0.91(5)	2.33(6)	2.972(5)	128(4)
N1–H1C···F1[1]	0.91(5)	2.52(5)	3.263(5)	139(4)

[a] Symmetry transformations used to generate equivalent atoms: a: $x, -y+1/2, z+1/2$; b: $x, y, z+1$; c: $x, -y+3/2, z+1/2$; 1: $-x, y-1/2, -z+3/2$; 3: $x, y-1, z$; 6: $x, -y+1/2, z-1/2$.

A comparison of the two structural types shows a couple of major differences. Firstly, when viewed down on the sheet, a triply bridging fluoride connecting two lithium centres in **1** and **2** aligns almost parallel to the *c* (*b*) axis producing the -[Li-F-Li-F-Li]- linear chain, whereas in **3** and **4** the same bridge lies perpendicular forming a zigzag effect running parallel to the *a* axis (Figure 3 c and d). Secondly, compounds **1** and **2**, when viewed down the *c* axis, display corner-sharing 4-nets, whereas in compounds **3** and **4** edge-sharing 4-nets are prevalent.

Conclusion

In general the layered-based 2D families of aluminophosphate[19, 20, 21] and zincophosphate,[22, 23] as well as the fluoride-based layered compounds reported in this paper, are very similar in nature because they all contain arrays of corner-sharing tetrahedra. A vast number of tetrahedral-based layers have been published and even more have been hypothesised to exist.

The aluminophosphate-based materials resemble the materials reported here with regard to the style of stacking which is manipulated by the presence of templating agents in the inter-layer regions that interact with the inorganic framework through extensive hydrogen bonds. Larger ring sizes are much more common in silicate and phosphate compounds such as in $[C_5N_2H_9]_2[NH_4]\cdot Al_3P_4O_{16}$ (4- and 6-nets),[24] $[NH_3CHMeCH_2NH_3]_3\cdot[Al_3P_4O_{16}]_2\cdot H_2O$ (4-, 6- and 8-nets)[25] and even 12-rings are found in the same anionic network templated by $[BuNH_3]^{2+}$.[26] The largest ring size observed so far in the compact $LiBeF_n$ layers are 4-rings, only when 3D materials are synthesised do larger ring sizes emerge, such as 6- and 8-rings.[27]

The presence of bridging and terminal M=O, M–OH and $M-OH_2$ groups complicate the picture somewhat from truly oxide-based materials. The aluminophosphates, mainly the $[Al_3P_4O_{16}]^{3-}$ layered family, show similar packing arrangements, to the fluoride-based materials, due to terminal P=O motifs (i.e. terminal Be–F bond in compounds **1**–**4**) that lie above and below the plane of the sheets, as observed in references [24–26]. These compounds form strong hydrogen bonds to the organoamine structure-directing templates in a similar fashion to the fluoride-based sheets discussed herein.

We have now reported several new 2D sheet structures built from linked LiF_4 and BeF_4 tetrahedra templated with organoamines. These materials show that by changing the size and shape of templating agents, compounds that display different topologies, with the same connectivity, can be synthesised. There are many theoretical tetrahedral-based structural topologies with edge- and, or, vertex-sharing triply bridging anionic species. Only a few oxygen-based materials formed from tetrahedral units and containing a triply bridging species are known; one is hemimorphite, $Zn_4(OH)_2Si_2O_7\cdot H_2O$,[28] which consists of puckered hexagonal nets of directly bonded Zn, Si and O atoms. The triply bridging oxide unit bridges two zinc and one silicon atom forming a 2D layered topology. The

three bond lengths to the triply bridging oxide are ~1.95 Å, for both Zn–O, and ~1.62 Å, for Si–O.

In comparison with metal–oxygen bonds (e.g. Si^{4+}–O^{2-}, Zn^{2+}–O^{2-}) the monovalent fluoride ion interaction to M^{2+} and particularly M^{+} metallo-centres is relatively weak. Hence in the compounds studied the presence of the triply bridging fluoride with two Li–F and one Be–F interaction is prevalent. The inclusion of triply bridging fluoride ions is unique to these types of materials reported herein; a thorough literature search has showed up no other materials of this type. However, a number of fluoride-based systems have been synthesised by O'Hare et al. but these materials are based on the chemistry of the actinides, and therefore higher metallic coordination geometry is observed. A few examples include, $[C_5N_2H_{14}][ThF_6]\cdot 0.5\,H_2O$,[29] a thorium/fluoride-based chain that has a 2-methylpyrazine organoamine template and is composed of face-sharing nine-coordinate tricapped trigonal-prismatic $[ThF_9]$ units. A second example, $[C_4N_2H_{12}]_2[U_2F_{12}]\cdot H_2O$,[30] has a 1D structure built up from edge-sharing polyhedra with the chains separated by piperazinium cations and solvent water molecules.

Altering the geometry of the organoamine template may afford higher dimensional materials with topologies resembling those of zeolites. To increase dimensionality it will be necessary to connect the sheets together through the terminal fluoride ions. Possible methods of achieving this aim would be i) the use of a higher ratio of metal in the reaction, ii) further reaction of the product with extra metal salts or iii) using templates with a greater number of amine functional groups.

Experimental Section

$[LiBeF_4][C_6H_4(CH_3)CH_2NH_3]$ (1), $[LiBeF_4][C_6H_4CH_2NH_3Cl]$ (2) and $[LiBeF_4][C_6H_5CH_2CH_2CH_2NH_3]$ (4): Beryllium fluoride (0.1 g, 0.002 mol), 30% hydrofluoric acid (0.085 mL, 0.002 mol) and lithium carbonate (0.035 g, 0.002 mol) were dissolved in distilled water (1 mL). 3-Methylbenzylamine (for **1**; 0.27 mL, 0.002 mol), 4-chlorobenzylamine (for **2**; 0.26 mL, 0.002 mol), or 3-phenyl-1-propylamine (for **4**; 0.3 mL, 0.002 mol) was added to give an overall molar ratio of 1:1:1:1 for BeF_2:HF:Li_2CO_3:[A] where A = 3-methylbenzylamine, 4-chlorobenzylamine and 3-phenyl-1-propylamine, respectively. The mixture was sealed in a 23 mL Teflon-lined Parr autoclave and heated at 180 °C for seven days. After the mixture was cooled, the title compound crystallised to form colourless block crystals for **1**, or colourless plates for both **2** and **4**, that were recovered by filtration and air-dried. **1**: Elemental analysis calcd (%) for $LiBeF_4C_8NH_{12}$: C 44.87, H 5.65, N 6.54; found C 44.51, H 5.55, N 6.64; selected IR absorption bands (KBr disc 4000–400 cm^{-1}): (N–H)/(C–H)/(C=C)/(C–C)/(C–N): $\tilde{\nu}$ = 3024 s, 2774 w, 2678 w, 1642 m, 1629 s, 1592 s, 1563 m. **2**: Elemental analysis calcd (%) for $LiBeF_4C_7NH_9Cl$: C 47.10, H 6.18, N 6.14; found C 47.34, H 6.22, N 6.14; selected IR absorption bands (KBr disc 4000–400 cm^{-1}): (N–H)/(C–H)/(C=C)/(C–C)/(C–N): $\tilde{\nu}$ = 3027 s br, 2785 w, 2664 w, 1648 m br, 1596 m, 1563 m, 1533 m, 1492 m, 1448 m, 1412 m, 1374 m. **4**: Elemental analysis calcd (%) for $LiBeF_4C_9NH_{14}$: C 47.10, H 6.18, N 6.14; found C 47.11, H 5.98, N 6.22; selected IR absorption bands (KBr disc 4000–400 cm^{-1}): (N–H)/(C–H)/(C=C)/(C–C)/(C–N): $\tilde{\nu}$ = 3510 m, 3442 m, 2999 s br, 2728 w, 2587 w, 2434 w, 2311 w, 2018 w, 1593 m, 1482 s, 1454 s, 1397 m, 1145 m.

$[LiBeF_4]_2[C_3N_2H_{12}]$ (3): Beryllium fluoride (0.1 g, 0.002 mol), 30% hydrofluoric acid (0.17 mL, 0.004 mol) and 1,3-diaminopropane (0.17 mL, 0.002 mol) were dissolved in distilled water (1 mL) to give an overall molar ratio of 1:2:1 for BeF_2:HF:[A] where A = 1,3-diaminopropane. The mixture was sealed in a 23 mL Teflon-lined Parr autoclave and heated at 150 °C for 2 h. After the mixture had been cooled, lithium carbonate (0.035 g, 0.002 mol) was dissolved into the solution and the mixture left to slowly evaporate. The title compound crystallised to form small colourless block crystals that were recovered by filtration and air-dried. **3**: Elemental analysis calcd (%) for $Li_2Be_2F_8C_3N_2H_{12}$: C 13.86, H 4.65, N 10.08; found C 13.88, H 4.96, N 9.96; selected IR absorption bands (KBr disc 4000–400 cm^{-1}): (N–H)/(C–H)/(C–C)/(C–N): $\tilde{\nu}$ = 3071 m br, 3007 m br, 2771, 2688, 2560, 2404, 1610 m, 1599 w, 1478 w, 1463 w, 1408 w, 1216 w, 1188 w, 1102 w.

X-ray crystallographic study: The crystal structures were determined from single-crystal X-ray diffraction data. Data were collected on a Nonius Kappa CCD Area detector diffractometer by using $Mo_{K\alpha}$ radiation (λ = 0.71073 Å) ω and ϕ scans to fill the Ewald sphere at 120(2) K. The crystal structure parameters are described in Table 5. The structures were solved by direct methods using SHELXS-97[15] and structure refinement by least-squares method SHELXL-97.[15] All the calculations were performed by using the WINGX[16] system (Ver 1.64.03). All the non-hydrogen atoms were refined anisotropically. Selected bond lengths and angles are listed in Table 1 and Table 2.

Thermal analysis: The thermal stability of compounds **1**, **2**, **3** and **4** were investigated by using TGA/DTA in air between 25 °C and 500 °C. Compound **1** showed a total mass loss of 55%, that is assigned to a possible loss of just the amine template and HF in two stages, around 200–400 °C. Compound **2** showed a total mass loss of 67%, that is assigned to a loss of the amine template and HF in three stages, again around 200–400 °C. Compound **3** showed a total mass loss of 52%, that is assigned to a loss of the amine template and HF and water, around 100–400 °C. Note this compound is slightly hydrophillic and picks up surface water. Compound **4** showed a total mass loss of 68%, that is assigned to a loss of the amine template and HF in three stages, around 150–400 °C.

CCDC-206718–206721 contain the supplementary crystallographic data for this paper. These data can be obtained free of charge via www.ccdc.cam.ac.uk/conts/retrieving.html (or from the Cambridge Crystallographic Data Centre, 12, Union Road, Cambridge CB2 1EZ, UK; fax: (+44) 1223-336-033; or deposit@ccdc.cam.ac.uk).

Table 5. Crystal data for **1**–**4**.

Empirical formula	$LiBeF_4C_8NH_{12}$ (**1**)	$LiBeF_4C_7NH_9Cl$ (**2**)	$Li_2Be_2F_8C_3N_2H_{12}$ (**3**)	$LiBeF_4C_9NH_{14}$ (**4**)
Fw	214.14	234.55	168.10	228.16
space group	P*ca*2(1)	P*bca*	P*ccn*	P2(1)/*c*
Z	4	8	4	4
T [K]	120(2)	120(2)	120(2)	120(2)
a [Å]	7.2491(2)	7.1613(7)	21.057(2)	21.557(3)
b [Å]	21.0877(7)	6.5965(5)	4.8117(4)	4.8469(7)
c [Å]	6.6169(2)	41.372(4)	9.8727(8)	10.0565(18)
V [Å^3]	1011.50(5)	1954.4(3)	1000.3(1)	1050.4(3)
μ [mm^{-1}]	0.131	0.408	0.117	0.131
ρ_{calcd} [Mg m^{-3}]	1.406	1.594	1.116	1.443
R_{int}	0.0522	0.1120	0.1004	0.0896
$R1$ [$I > 2\sigma(I)$]	0.0420	0.0663	0.0453	0.0661
$wR2$ [$I > 2\sigma(I)$]	0.1001	0.1282	0.0889	0.1572
data/restraints/parameters	2314/1/172	1599/0/155	1050/0/103	1502/0/201

Acknowledgements

We thank Prof. M. B. Hursthouse for access to the Kappa CCD diffractometer, Medac for the microanalysis and the EPSRC for funding under GR/R12077.

[1] a) R. C. Haushalter, L. A. Mundi. *Chem. Mater.* **1992**, *4*, 31; b) R. M. Barrer, *Zeolites*, **1981**, *1*, 130.
[2] S. A. Schunk, L. Schüth, *Molecular Sieve Science and Technology*, Springer, Berlin, **1998**, *1*, 229.
[3] S. T. Wilson, B. M. Lok, C. A. Messina, T. R. Cannan, E. M. Flanigen, *J. Am. Chem. Soc.* **1982**, *104*, 1146.
[4] J. Yu, R. Xu, *Acc. Chem. Res.* **2003**, *36*, 481.
[5] C. T. Kresge, M. E. Leonowicz, W. J. Roth, J. C. Vartuli, J. S. Beck, *Nature*, **1992**, *359*, 710.
[6] B. G. Shpeizer, P. Sylvester, R. A. Cahill, A. Clearfield, *Chem. Mater.* **1999**, *11*, 1201.
[7] W. Chen, Y. S. Jiang, H. Huo, H. M. Yuan, J. S. Chen, *Chinese Chem. Lett.* **2002**, *13*, 5, 474.
[8] a) A. Tuel, V. Gramlich, C. Baerlocher, *Microporous Mesoporous Mater.* **2001**, *47*, 2–3, 217; b) K. X. Wang, J. H. Yu, P. Miao, Y. Song, J. Y. Li, Z. Shi, R. R. Xu, *J. Mater. Chem.* **2001**, *11*, 7, 1898.
[9] a) K. X. Wang, J. H. Yu, Z. Shi, P. Miao, W. F. Yan, R. R. Xu, *J. Chem. Soc. Dalton*, **2001**, 1809; b) K. Maeda, A. Tuel, S. Caldarelli, C. Baerlocher, *Microporous Mesoporous Mater.* **2000**, *39*, 3, 465.
[10] L. Vidal, C. Pray, J. Patarin, *Microporous Mesoporous Mater.* **2000**, *39*, 1–2, 113.
[11] L. Sierra, J. Patarin, J. L. Guth, *Microporous Mesoporous Mater.* **2000**, *38*, 2–3, 123.
[12] B. Wei, J. H. Yu, Z. Shi, S. L. Qiu, J. Y. Li, *J. Chem. Soc. Dalton*. **2000**, 1979.
[13] L. A. Gerrard, M. T. Weller, *Chem. Commun.* **2003**, 716.
[14] L. A. Gerrard, M. T. Weller, *J. Chem. Soc. Dalton Trans.* **2002**, *23*, 4402.
[15] Programs for Crystal Structure Analysis (Release 97–2). G. M. Sheldrick, Institüt für Anorganische Chemie der Universität, Tammanstrasse 4, 3400 Göttingen, Germany, **1998**.
[16] L. J. Farrugia, WINGX suite, *J. Appl. Crystallogr*. **1999**, *32*, 837–838.
[17] J. C. Tedenac, S. Vilminot, L. Cot, A. Corbert, M. Maurin, *Mater. Res. Bull.* **1971**, *6*, 183.
[18] I. D. Williams, Q. Gao, J. Chen, J. Yu, R. Xu, *Chem. Commun*. **1997**, *14*, 1273.
[19] A. Chippindale, R. I. Walton, *J. Solid State Chem.* **1999**, *145*, 731.
[20] P. S. Wheatley, C. J. Love, J. J. Morrison, I. J. Shannon, R. E. Morris, *J. Mater. Chem.* **2002**, *12*, 477.
[21] W. F. Yan, J. H. Yu, Y. Li, Z. Shi, R. R. Xu, *J. Solid State Chem.*, **2002**, *167*, 282.
[22] S. Natarajan, *Inorg. Chem.* **2002**, *41*, 5530–5537.
[23] Y. L. Liu, W. Liu, Y. Xing, Z. Shi, Y. L. Fu, W. Q. Pang, *J. Solid State Chem.* **2002**, *166*, 265.
[24] J. Yu, J. Li, K. Sugiyama, N. Togashi, O. Terasaki, K. Hiraga, B. Zhou, S. Qiu, R. Xu, *Chem. Mater.* **1999**, *11*, 1727.
[25] I. D. Williams, Q. Gao, J. Chen, L-Y. Ngai, Z. Lin, R. Xu, *Chem. Commun*. **1996**, *15*, 1781.
[26] A. M. Chippindale, A. R. Cowley, Q. Huo, R. H. Jones, A. D. Law, *J. Chem. Soc. Dalton Trans.* **1997**, 2639.
[27] M. R. Anderson, I. D. Brown, S. Vilminot, *Acta Crystallogr. Sect. B* **1973**, *29*, 2625.
[28] E. Libowitzky, A. J. Schultz, D. M. Young, *Z. Kristallogr.*, **1998**, *213*, 659.
[29] J-Y. Kim, A. J. Norquist, D. O'Hare, *Chem. Commun*. **2002**, *19*, 2198.
[30] S. M. Walker, P. S. Halasyamani, S. Allen, D. O'Hare, *J. Am. Chem. Soc.* **1999**, *121*, 10513.

Received: March 25, 2003 [F4991]